Inorganic Chemistry
Article

*Inorg. Chem.* **2009**, *48*, 8445–8455 **8445**
DOI: 10.1021/ic901062n

# Photoinduced Release of $Zn^{2+}$ with ZinCleav-1: a Nitrobenzyl-Based Caged Complex

**H. M. Dhammika Bandara,[†] Daniel P. Kennedy,[†] Elif Akin,[†] Christopher D. Incarvito,[‡] and Shawn C. Burdette*[,†]**

[†]*Department of Chemisty, University of Connecticut, 55 North Eagleville Road U- 3060, Storrs, Connecticut 06269, and* [‡]*Department of Chemistry, Yale University, 225 Prospect Street, P.O. Box 208107, New Haven, Connecticut 06520-8107*

Received June 2, 2009

Caged complexes are metal ion chelators that release analytes when exposed to light of a specific wavelength. The synthesis and properties of ZinCleav-1, a cage for $Zn^{2+}$ that fragments upon photolysis, is reported. The general uncaging strategy involves integrating a nitrobenzyl group on the backbone of the ligand so that a carbon-heteroatom bond is cleaved by the photoreaction. The caged complex was obtained using a new synthetic strategy involving a Strecker synthesis to prepare a key aldehyde intermediate. ZinCleav-1 has a $K_d$ of 0.23 pM for $Zn^{2+}$ as measured by competitive titration with $[Zn(PAR)_2]$ (PAR = 4-(2-pyridyl-2-azo) resorcinol). The quantum yield for ZinCleav-1 is 2.4% and 0.55% for the apo and $Zn^{2+}$ complex, respectively. The ability of ZinCleav-1 to increase free $[Zn^{2+}]$ is calculated theoretically using the binding constants for the uncaged photoproducts, and demonstrated practically by using a fluorescent sensor to image the liberated $Zn^{2+}$. Free $Zn^{2+}$ may function as a neurotransmitter and have a role in the pathology of several neurological diseases. Studying these physiological functions remains challenging because $Zn^{2+}$ is silent to most common spectroscopic techniques. We expect ZinCleav-1 to be the first in a class of caged complexes that will facilitate biological investigations.

## Introduction

Delineating the trafficking and function of bioactive molecules and metal ions at the cellular level remains challenging; however, there are a number of chemical tools that have emerged to facilitate these investigations. Fluorescent sensors were developed by Roger Tsien and others to elucidate intracellular signaling pathways of $Ca^{2+}$,[1] and recently similar technologies have been reported for $Zn^{2+}$.[2] In addition to fluorescent sensors, caged complexes for $Ca^{2+}$ were developed concurrently with sensors.[3,4] A caged metal complex is a chelator that undergoes a photochemical reaction that modulates its binding affinity. Using the combination of sensors to image endogenous metal ions and caged complexes to control the release of metal ions can provide insight into biological phenomena that are not accessible using each independently. While numerous sensors have been reported, caged complexes for $Zn^{2+}$ have not been developed to date.

To facilitate $Zn^{2+}$ signaling research, we have designed, prepared, and characterized ZinCleav-1, a chelating ligand with four donor groups that is fractured into two fragments with two donor atoms each upon exposure to light (Figure 1). Cleaving a covalent bond provides a powerful methodology to change binding affinity through reduction of chelate effects. Existing complexes for $Ca^{2+}$ and $Cu^{2+}$ utilize a similar uncaging strategy;[4,5] however, accessing a diverse variety of caged chelators via these routes is limited because of synthetic restrictions. To thoroughly investigate $Zn^{2+}$ signaling pathways, cages will be needed with structures that will allow a wide range of free metal concentrations to be generated.

Almost 50 years have passed since stainable (i.e., free or chelatable) zinc was discovered in the brain,[6] and over 30 years since the concept of synaptic zinc was introduced to the neuroscience community.[7,8] In 1967, Haug demonstrated that this pool of zinc was contained in the vesicles of presynaptic nerve terminals in the hippocampus,[9] and since that time the function of free zinc has been the subject of considerable interest, scrutiny, and controversy. Zinc-containing neurons are characterized as possessing weakly bound zinc in the vesicles of their presynaptic boutons, vesicles that also contain glutamate.[10] Zinc meets three

*To whom correspondence should be addressed. E-mail: shawn.burdette@uconn.edu.

(1) Tsien, R. Y. *Annu. Rev. Neurosci.* **1989**, *12*, 227–253.
(2) Jiang, P.; Guo, Z. *Coord. Chem. Rev.* **2004**, *248*, 205–229.
(3) Tsien, R. Y.; Zucker, R. S. *Biophys. J.* **1986**, *50*, 843–853.
(4) Ellis-Davies, G. C. R.; Kaplan, J. H. *J. Org. Chem.* **1988**, *53*, 1966–1969.
(5) Ciesienski, K. L.; Haas, K. L.; Dickens, M. G.; Tesema, Y. T.; Franz, K. J. *J. Am. Chem. Soc.* **2008**, *130*, 12246–12247.
(6) Maske, H. *Naturwissenschaften* **1955**, *42*, 424.
(7) McLardy, T. *Confin. Neurol.* **1960**, *20*, 1–19.
(8) McLardy, T. *Acta Neurochir.* **1970**, *23*, 119–124.
(9) Haug, F. M. *Histochemie* **1967**, *8*, 355–368.
(10) Beaulieu, C.; Dyck, R.; Cynader, M. *Neuroreport* **1992**, *10*, 861–864.


Published on Web 07/27/2009

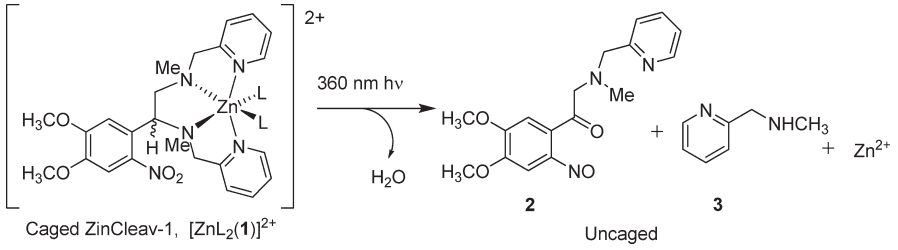


**Figure 1.** Uncaging action of ZinCleav-1. Upon irradiation, the nitrobenzyl group abstracts a hydrogen atom to initiate a reaction cascade that cleaves the adjacent carbon−nitrogen bond. The ZinCleav nomenclature refers to the bond cleavage step, which releases $Zn^{2+}$. L corresponds to solvent molecules.

requirements that suggest an analyte as a possible neuromodulator including (1) a regulatory system for introducing $Zn^{2+}$ into neurons, (2) the ability for $Zn^{2+}$ to be released from presynaptic vesicles and modulate postsynaptic neurotransmitter receptors, and (3) processes that are capable of stopping the signal.[11]

Although the presence of synaptic $Zn^{2+}$ provides circumstantial evidence for the existence of zinc-dependent neurological processes, the exact signaling pathways of physiological significance, and the concentration required to initiate activity remain controversial. Original estimates of the maximum concentration of $Zn^{2+}$ available for signaling were as high as 300 $\mu$M;[12] however, others have suggested that minimal synaptic $Zn^{2+}$ is released.[13] The latter report has been disputed in many other reports.[14−16] While $Zn^{2+}$ can be released from synaptic vesicles by electrical stimulation,[17] or applied exogenously in the form of a $Zn^{2+}$ salt in the presence[18] or absence[19] of a $Zn^{2+}$ ionophore, these techniques often overwhelm a system with ionic $Zn^{2+}$. Lack of methods for controlled $Zn^{2+}$ release is a problem because observations made using existing techniques might suggest $Zn^{2+}$ can provoke certain biological responses, although the concentration required to initiate the activity is not physiologically relevant. Caged $Zn^{2+}$ complexes could help resolve this discrepancy about the relevance of $Zn^{2+}$ to synaptic transmission.

## Experimental Section

**General Synthetic Procedures.** All reagents were purchased from Acros at the highest commercial quality and used without further purification unless otherwise stated. *N*-methyl-2-(aminomethyl)pyridine (**3**),[20] amino-(3,4-dimethoxy-phenyl)-acetic acid (**6**),[21] ethylene-bis-α,α′-(2-aminomethyl)pyridine (EBAP, **15**),[22] *N*,*N*′-dimethyl-*N*,*N*′-bis-(pyridin-2-ylmethyl)-ethane-1,2-diamine (DM-EBAP, **16**)[23], and 2-bromo-1-(3,4-dimethoxy-phenyl)-ethanone (**19**)[24] were synthesized according to literature procedures. Dichloromethane ($CH_2Cl_2$), toluene ($C_6H_5CH_3$), and tetrahydrofuran (THF) were sparged with argon and dried by passage through a Seca Solvent Purification System. All chromatography and thin-layer chromatography (TLC) were performed on silica (230−400 mesh) from Silicycle unless otherwise specified. TLCs were developed with mixtures of $CH_2Cl_2$/$CH_3OH$ or $CH_2Cl_2$/$CH_3OH$/$NH_4OH$ unless otherwise specified and were visualized with 254 and 365 nm light. $^1H$ and $^{13}C$ NMR spectra were recorded using a Bruker 400 MHz NMR instrument, and chemical shifts are reported in ppm on the $\delta$ scale relative to tetramethylsilane. IR spectra were recorded on a Nicolet 205 FT-IR instrument, and the samples were prepared as KBr pellets or thin films on KBr plates. High resolution mass spectra were recorded at the University of Connecticut mass spectrometry facility using a micromass Q-Tof-2 mass spectrometer operating in positive ion mode. Elemental analysis was acquired with an Elementar combustion analyzer.

**Amino-(3,4-dimethoxy-phenyl)-acetic Acid Methyl Ester (7).** The aminoacid **6** (10.0 g, 47.3 mmol) and *p*-toluenesulfonic acid monohydrate (18.9 g, 99 mmol) were combined in methanol (165 mL) and refluxed for 24 h. The solvent was removed, and the resulting solid was dissolved in 30% $NH_4OH$ (80 mL) and extracted with $CH_2Cl_2$ (3 × 100 mL). The organic layer was dried over $MgSO_4$, and the solvent removed under vacuum to yield **7** as a brown solid (9.12 g, 84.1%). TLC $R_f$ = 0.44 (silica, 24:1 $CH_2Cl_2$:$CH_3OH$). Mp = 37−38 °C . $^1H$ NMR (400 MHz, $CDCl_3$) $\delta$ 6.61 −6.74 (m, 3H), 4.34 (s, 1H), 3.65 (s 3H), 3.63 (s, 3H), 3.46 (s, 3H), 1.87 (s, 2H). $^{13}C$ NMR (100 MHz, $CDCl_3$) $\delta$ 174.2, 148.8, 148.5, 132.6, 118.8, 110.9, 58.0, 55.5, 51.9. IR (KBr pellet, $cm^{-1}$) 3350.7, 3001.6−2927.4, 2835.8, 1738.5, 1605.4, 1520.6, 1466.6, 1025.0. HRMS (+ESI): Calcd. for $MH^+$, 226.1079; Found 226.1128.

**[1-(3,4-Dimethoxy-phenyl)-2-hydroxy-ethyl]-carbamic Acid *tert*-Butyl Ester (9).** The aminoester **7** (9.0 g, 39.9 mmol) and triethylamine (11.1 mL, 79.9 mmol) were combined in $CH_2Cl_2$ (200 mL) and di-*tert*-butyl dicarbonate (9.58 g, 43.9 mmol) was added. The reaction mixture was stirred at 23 °C for 24 h and then washed sequentially with 1 M HCl (100 mL), sat. $NaHCO_3$ (100 mL) and water (100 mL). The organic solution was dried over $MgSO_4$, and the solvent was removed to yield *tert*-butoxycarbonylamino-(3,4-dimethoxy-phenyl)-acetic acid methyl ester (**8**) as a colorless oil (12.8 g), which was used in the next step without further purification. The product **8** (12.8 g, mmol) was dissolved in THF (50 mL), and $NaBH_4$ (4.53 g, 120 mmol), LiCl (5.04 g, 120 mmol) and EtOH (100 mL) were added. The resulting mixture was stirred at 23 °C for 20 h. The reaction was quenched by adding water (30 mL). The product was extracted into $CH_2Cl_2$ (3 × 100 mL), and the combined organic extracts were dried over $MgSO_4$. Flash chromatography on silica (49:1 $CH_2Cl_2$/$CH_3OH$) yielded **9** as a white solid (8.20 g, 69.1%). TLC

(11) Smart, T. G.; Hosie, A. M.; Miller, P. S. *Neuroscientist* **2004**, *10*, 432–442.
(12) Assaf, S. Y.; Chung, S.-H. *Nature* **1984**, *308*, 734–736.
(13) Kay, A. R. *J. Neurosci.* **2003**, *23*, 6847–6855.
(14) Frederickson, C. J.; Giblin, L. J.; Rengarajan, B.; Masalha, R.; Frederickson, C. J.; Zeng, Y. P.; Lopez, E. V.; Koh, J. Y.; Chorin, U.; Besser, L.; Hershfinkel, M.; Li, Y.; Thompson, R. B.; Krezel, A. *J. Neurosci. Methods* **2006**, *154*, 19–29.
(15) Takeda, A.; Kanno, S.; Sakurada, N.; Ando, M.; Oku, N. *J. Neurosci. Res.* **2008**, *86*, 2906–2911.
(16) Takeda, A.; Sakurada, N.; Kanno, S.; Minami, A.; Oku, N. *J. Neurochem.* **2006**, *99*, 670–676.
(17) Cole, T. B.; Martyanova, A.; Palmiter, R. D. *Brain Res.* **2001**, *891*, 253–265.
(18) Haase, H.; Maret, W. *Exp. Cell Res.* **2003**, *291*, 289–298.
(19) Pifl, C.; Rebernik, P.; Kattinger, A.; Reither, H. *Neuropharm.* **2004**, *46*, 223–231.
(20) Seitz, M.; Kaiser, A.; Tereshchenko, A.; Geiger, C.; Uematsu, Y.; Reiser, O. *Tetrahedron* **2006**, *62*, 9973–9980.
(21) Kehayova, P. D.; Bokinsky, G. E.; Huber, J. D.; Jain, A. *Org. Lett.* **1999**, *1*, 187–188.
(22) Lacoste, R. G.; Marttel, A. E. *Inorg. Chem.* **1964**, *3*, 881–884.
(23) White, M. C.; Doyle, A. G.; Jacobsen, E. N. *J. Am. Chem. Soc.* **2001**, *123*, 7194–7195.
(24) Jacob, J. N.; Nichols, D. E.; Kohli, J. D.; Glock, D. *J. Med. Chem.* **1981**, *24*, 1013–1015.

$R_f$ = 0.58 (silica, 24:1 $CH_2Cl_2$:$CH_3OH$). Mp = 76−77 °C. $^1$H NMR (400 MHz, $CDCl_3$) $\delta$ 6.85 (s, 2H), 6.83 (s, 1H), 5.26 (s, 1H), 4.70 (s, 1H), 3.88 (s, 3H), 3.87 (s, 3H), 3.82 (s, 2H), 2.56 (s, 1H), 1.44 (s, 9H). $^{13}$C NMR (100 MHz, $CDCl_3$) $\delta$ 156.1, 149.2, 148.6, 132.1, 118.6, 111.4, 110.0, 80.0, 66.8, 56.7, 56.0, 55.9, 28.3 ppm; IR (KBr pellet, $cm^{-1}$) 3371.9, 2985.3−2836.8, 1688.4, 1527.3, 1465.6, 1264.1, 1169.6, 1027.9. HRMS (+ESI): Calcd. for $MH^+$, 320.1474; Found, 320.1505.

**[1-(3,4-Dimethoxy-phenyl)-2-(methyl-pyridin-2-ylmethyl-amino)-ethyl]-carbamic Acid *tert*-Butyl Ester (11).** Dess-Martin periodinane (3.14 g, 7.40 mmol) was suspended in $CH_2Cl_2$ (60 mL), and a solution of **9** (2.00 g, 6.73 mmol) in $CH_2Cl_2$ (30 mL) was added. The mixture was stirred at 23 °C for 18 h. The resulting reaction mixture was diluted with $Et_2O$ (90 mL) and quenched by adding a solution of $Na_2S_2O_3 \cdot 5H_2O$ (51.8 mmol) in saturated $NaHCO_3$ (30 mL). The product was extracted into $CH_2Cl_2$ (3 × 100 mL), the organic layer was dried over $MgSO_4$ and then evaporated to yield [1-(3,4-dimethoxy-phenyl)-2-oxo-ethyl]-carbamic acid *tert*-butyl ester (**10**) as a brown oil (1.65 g, 83.1%), which was used in the next step without purification. The oil **10** (1.65 g) was dissolved in $CH_2Cl_2$ (50 mL) and treated sequentially with **3** (683 mg, 5.59 mol), glacial AcOH (0.32 mL, 5.59 mmol) and $NaBH(OAc)_3$ (1.78 g, 8.39 mmol). The solution was stirred at 23 °C for 24 h. Saturated $Na_2CO_3$ (30 mL) was added to the reaction mixture, and the product was extracted in to $CH_2Cl_2$ (3 × 60 mL). The combined organic extracts were dried over $MgSO_4$, and the solvent was removed. Flash chromatography on silica (24:1 $CH_2Cl_2$/$CH_3OH$) yielded **11** as a yellow oil (1.71 g, 63.4%). TLC $R_f$ = 0.32 (silica, 24:1 $CH_2Cl_2$:$CH_3OH$). $^1$H NMR (400 MHz, $CDCl_3$) $\delta$ 8.57 (d, $J$ = 5.1 Hz, 1H), 7.64 (td, $J$ = 1.7, 7.7, 1H), 7.31 (d, $J$ = 7.7 Hz, 1H), 7.18 (dd, $J$ = 5.1, 7.7 Hz, 1H), 6.81 (s, 2H), 6.78 (s, 1H), 5.94 (s, 1H), 4.62 (s, 1H), 3.85 (s, 3H), 3.84 (s, 3H), 3.80 (d, $J$ = 15.0 Hz, 1H), 3.66 (d, $J$ = 15.0 Hz, 1H), 2.61 (m, 2H), 2.35 (s, 3H), 1.41 (s, 9H). $^{13}$C NMR (100 MHz, $CDCl_3$) $\delta$ 159.1, 149.1, 149.0, 148.3, 136.5, 135.2, 123.1, 122.1, 119.0, 111.0, 110.0, 65.6, 63.9, 56.0, 55.9, 53.2, 42.7. IR (thin film, $cm^{-1}$) 3378.7, 3008.4−2815.5, 1714.4, 1518.7, 1261.2, 1171.5, 1030.8; HRMS (+ESI): Calcd. for $MH^+$, 402.2393; Found, 402.2403.

**1-(3,4-Dimethoxy-phenyl)-*N*′-methyl-*N*′-pyridin-2-ylmethyl-ethane-1,2-diamine (12).** Trifluoroacetic acid ($CF_3CO_2H$, 8 mL) was added to a solution of **11** (1.60 g, 3.99 mmol) in $CH_2Cl_2$ (40 mL) and stirred at 23 °C for 24 h. After removing the solvent, saturated $K_2CO_3$ (30 mL) was added to the reaction mixture, and the product was extracted into $CH_2Cl_2$ (3 × 60 mL). The combined organic extracts were dried over $MgSO_4$, and the solvent was removed to yield **12** as a brown oil (1.12 g, 93.1%). TLC $R_f$ = 0.48 (basic alumina, 24:1 $CH_2Cl_2$:$CH_3OH$). $^1$H NMR (400 MHz, $CDCl_3$) $\delta$ 8.40 (d, $J$ = 5.0 Hz, 1H), 7.60 (td, $J$ = 1.7, 7.6 Hz, 1H), 7.33 (d, $J$ = 7.6 Hz, 1H), 7.10 (dd, $J$ = 5.0, 7.6 Hz, 1H), 7.00 (d, $J$ = 1.8 Hz, 1H), 6.87 (dd, $J$ = 1.8, 8.2 Hz, 1H), 6.78 (d, $J$ = 8.2 Hz, 1H), 4.11 (dd, $J$ = 3.7, 10.4 Hz, 1H), 3.95 (br s, 2H), 3.84 (s, 3H), 3.82 (s, 3H), 3.75 (d, $J$ = 14.0 Hz, 1H), 3.69 (d, $J$ = 14.0 Hz, 1H), 2.76 (dd, $J$ = 10.4, 12.5 Hz, 1H), 2.51 (dd, $J$ = 3.7, 12.5 Hz, 1H), 2.31 (s, 3H). $^{13}$C NMR (100 MHz, $CDCl_3$) $\delta$ 159.1, 149.1, 149.0, 148.3, 136.5, 135.2, 123.1, 122.1, 119.0, 111.0, 110.0, 65.5, 63.9, 56.0, 55.9, 53.2, 42.7. IR (thin film, $cm^{-1}$) $\nu$ 3380.6, 3309.2, 3059.5−28.15.5, 1592.9, 1519.6, 1466.6, 1268.0, 1145.5, 1030.8. HRMS (+ESI): Calcd. for $MH^+$, 302.1869; Found, 302.1846.

**1-(3,4-Dimethoxy-phenyl)-*N*′-methyl-*N*,*N*′-bis-pyridin-2-ylmethyl-ethane-1,2-diamine (13).** The diamine **12** (1.05 g, 3.48 mmol) and 2-pyridinecarboxaldehyde (0.33 mL, 3.48 mmol) were combined in EtOH (30 mL) and refluxed at 78 °C for 1 h. After the solution cooled to room temperature, $NaBH_4$ (132 mg, 3.48 mmol) was added, and the resulting mixture was stirred for 18 h at 23 °C. The crude reaction mixture was diluted with saturated $NaHCO_3$ (20 mL), and the product was extracted into $CH_2Cl_2$ (3 × 50 mL). The combined organic extracts were dried over $MgSO_4$, and the solvent was removed. Flash chromatography on silica (95:4:1 $CH_2Cl_2$/$CH_3OH$/$NH_4OH$) yielded **13** as a yellow oil (986 mg, 72.3%). TLC $R_f$ = 0.68 (basic alumina, 24:1 $CH_2Cl_2$:$CH_3OH$). $^1$H NMR (400 MHz, $CDCl_3$) $\delta$ 8.51 (m, 2H), 7.65 (m, 2H), 7.56 (m, 2H), 7.17−7.10 (m, 4H), 6.99 (d, $J$ = 1.8 Hz, 1H), 6.88 (dd, $J$ = 1.8, 8.2 Hz, 1H), 6.82 (d, $J$ = 8.2 Hz, 1H), 3.87 (s, 6H), 3.83−3.60 (m, 5H), 2.75 (dd, $J$ = 10.6, 12.1 Hz, 1H), 2.51 (dd, $J$ = 3.7, 12.1 Hz, 1H), 2.26 (s, 3H). $^{13}$C NMR (100 MHz, $CDCl_3$) $\delta$ 158.9, 155.8, 149.1, 149.0, 136.5, 134.9, 123.0, 122.1, 118.2, 111.2, 109.4, 79.1, 63.5, 63.2, 55.9, 55.8, 53.1, 42.7, 28.4. IR (thin film, $cm^{-1}$) 3319.8, 3007.4−2804.0, 1591.9, 1514.8, 1465.6, 1266.0, 1143.6, 1029.8; HRMS (+ESI): Calcd. for $MH^+$, 393.2291; Found, 393.2272.

**1-(3,4-Dimethoxy-phenyl)-*N*,*N*′-dimethyl-*N*,*N*′-bis-pyridin-2-ylmethyl-ethane-1,2-diamine (14).** The diamine **13** (951 mg, 2.42 mmol) was dissolved in 40 mL of $CH_3CN$/$CH_3OH$ (1:1) and $CH_2O$ (37% in water, 7.0 mL) was added. $NaBH_3CN$ (760 mg, 12.1 mmol) and AcOH (2.7 mL) were added, and the reaction mixture was stirred at 23 °C for 18 h. After the solvent was removed, saturated $NaHCO_3$ (20 mL) was added, and the product was extracted into $CH_2Cl_2$ (3 × 60 mL). The combined organic extracts were dried over $MgSO_4$, and the solvent was removed. Flash chromatography on silica (95:4:1 $CH_2Cl_2$/ $CH_3OH$/ $NH_4OH$) yielded **14** as a yellow oil (664 mg, 67.5%). TLC $R_f$ = 0.70 (basic alumina, 24:1 $CH_2Cl_2$:$CH_3OH$). $^1$H NMR (400 MHz, $CDCl_3$) $\delta$ 8.43 (m, 2H), 7.55 (m, 1H), 7.48−7.40 (m, 2H), 7.11 (d, $J$ = 8.4 Hz, 1H), 7.04 (m, 2H), 6.76 (s, 3H), 3.83 (s, 3H), 3.81 (s, 3H), 3.79−3.51 (m, 5H), 2.96 (d, 12.5 Hz, 1H), 2.80 (dd, $J$ = 3.7, 12.5 Hz, 1H), 2.23 (s, 3H), 2.12 (s, 3H). $^{13}$C NMR (100 MHz, $CDCl_3$) $\delta$ 160.3, 159.5, 148.8, 148.6, 148,5, 148.1, 136.3, 136.2, 132.1, 123.1, 122.8, 121.8, 121.7, 121.1, 111.9, 110.6, 65.9, 64.3, 60.6, 60.2, 55.8, 43.1, 38.9. IR (thin film, $cm^{-1}$) 3006.5−2801.1, 1591.0, 1517.7, 1472.4, 1262.2, 1149.4, 1030.8. HRMS (+ESI): Calcd. for $MH^+$, 407.2447; Found 407.2433.

**1-(4,5-Dimethoxy-2-nitro-phenyl)-*N*,*N*′-dimethyl-*N*,*N*′-bis-pyridin-2-ylmethyl-ethane-1,2-diamine (ZinCleav-1, 1).** Trifluoromethanesulfonic acid (TfOH, 0.16 mL, 1.84 mmol) was dissolved in $CH_2Cl_2$ (5 mL) and anhydrous $HNO_3$ acid (58 mg, 0.92 mmol) was added, which caused a white, crystalline solid to precipitate from the solution. After reducing the temperature of the reaction mixture to 0 °C, **14** (92 mg, 0.23 mmol) dissolved in $CH_2Cl_2$ (1 mL) was added in one portion. The reaction mixture was stirred at 0 °C for 1 h and then quickly poured onto 10 g of crushed ice. A saturated solution of $NaHCO_3$ (20 mL) was added, and the crude reaction mixture was extracted with $CH_2C1_2$ (3 × 30 mL). The combined organic extracts were dried over $MgSO_4$, and the solvent was removed. Flash chromatography on silica (95:4:1 $CH_2Cl_2$/$CH_3OH$/ $NH_4OH$) yielded ZinCleav-1 as a yellow oil (39.8 mg, 39.0%). TLC $R_f$ = 0.76 (basic alumina, 24:1 $CH_2Cl_2$:$CH_3OH$). $^1$H NMR (400 MHz, $CDCl_3$) $\delta$ 8.47 (m, 2H), 7.58 (td, $J$ = 1.7, 7.7 Hz, 1H), 7.46 (td, $J$ = 1.9, 7.6 Hz, 1H), 7.36 (s, 1H), 7.29 (d, $J$ = 7.6 Hz, 1H), 7.10−7.02 (m, 4H), 4.77 (d, $J$ = 10.6, 1H), 3.91 (s, 3H), 3.81 (s, 3H), 3.68 (d, $J$ = 15.0 Hz, 2H), 3.60 (d, $J$ = 15.0 Hz, 2H), 2.94 (d, $J$ = 12.0 Hz, 1H), 2.77 (dd, $J$ = 3.7, 12.0 Hz, 1H), 2.30 (s, 3H), 2.23 (s, 3H). $^{13}$C NMR (100 MHz, $CDCl_3$) $\delta$ 160.0, 159.4, 152.4, 149.2, 149.0, 147.7, 144.0, 136.8, 136.5, 131.0, 123.6, 122.8, 122.2, 111.0, 107.9, 65.0, 61.0, 60.4, 59.7, 56.6, 43.5, 40.0. IR (thin film, $cm^{-1}$) 3003.5−2809.1, 1598.1, 1557.3, 1517.7, 1501.9, 1478.4, 1270.3, 1151.4, 1020.8. HRMS (+ESI): Calcd. for $MH^+$, 452.2298; Found, 452.2279.

***N*,*N*′-dimethyl-*N*,*N*′-bis-(pyridin-2-ylmethyl)-ethane-1,2-diamine tetrahydrochoride (DM-EBAP·4HCl, 17).** A sample of 2-picholeyl chloride·HCl (3.0 g, 18.3 mmol) was treated with aqueous $K_2CO_3$ (5.0 g, 37 mmol), and the isolated free-base product (2.1 g, 16.5 mmol) was added to a solution of *N*,*N*′-dimethyl ethylenediamine (770 mg, 8.75 mmol) in $CH_2Cl_2$ (25 mL). A solution of 1 M NaOH (20 mL, 20 mmol) was added, and the mixture was stirred at room temperature for 60 h. The mixture was diluted with 1 M NaOH (20 mL), and the product

was extracted into $CH_2Cl_2$ (3 × 30 mL). After removal of solvent, flash chromatography on silica (88:10:2 $CH_2Cl_2$/$CH_3OH$/$NH_4OH$) yielded DM-EBAP as a brown oil (1.4 g, 60.1%). A 1.0 g sample of DM-EBAP was dissolved in a minimum amount of EtOH and treated with 10 mL of concentrated HCl. The resulting white precipitate was filtered off, and the filtrate was treated with excess $Et_2O$ to obtain more of the white precipitate. The precipitate was filtered off, washed with dry $Et_2O$ (3 × 20 mL), and dried under vacuum to yield 1.9 g of DM-EBAP·4HCl. TLC $R_f$ = 0.69 (basic alumina, 24:1 $CH_2Cl_2$:$CH_3OH$). $^1$H NMR (400 mHz, $CDCl_3$) $\delta$ 8.38 (m, 2H), 7.47 (m, 2H), 7.27 (d, $J$ = 10 Hz, 2H), 6.98 (m, 2H), 3.55 (s, 4H), 2.51 (s, 4H), 2.14)s, 6H). $^{13}$C NMR (100 MHz, $CDCl_3$) $\delta$ 159.6, 149.1, 136.4, 123.1, 121.9, 64.3, 55.7, 43.0. Anal. Calcd for $C_{14}H_{26}C_{l4}N_4$, C, 46.17; H, 6.30; Cl, 34.07; N, 13.46; Found C, 46.86; H, 6.44; Cl, 33.18; N, 13.52.

**1-(3,4-Dimethoxy-phenyl)-2-(methyl-pyridin-2-ylmethyl-amino)-ethanone (18).** A solution of **3** (400 mg, 1.54 mmol) in $C_6H_5CH_3$ (5 mL) was added dropwise to a vigorously stirring solution of **19** (226 mg, 1.85 mmol) and triethylamine (0.26 mL, 1.85 mmol) in $C_6H_5CH_3$ (5 mL). After completion of the addition the mixture was stirred and refluxed for 16 h at 111 °C. After cooling to room temperature, the reaction mixture was filtered to remove triethylamine hydrobromide, and the filtrate was extracted with several portions of dilute HCl. The pH of the combined aqueous extracts was adjusted to ~12 with 40% aqueous NaOH, and the resultant oil was extracted into $CH_2Cl_2$ (3 × 50 mL). After solvent removal, flash chromatography on silica (95:4:1 $CH_2Cl_2$/$CH_3OH$/ $NH_4OH$) yielded **17** as a brown oil (399 mg, 86.1%). $^1$H NMR (400 MHz, $CDCl_3$) $\delta$ 8.55 (d, $J$ = 7.6 Hz, 1H), 7.66−7.62 (m, 2H), 7.56 (d, $J$ = 1.7 Hz, 1H), 7.50 (dd, $J$ = 1.7, 7.2 Hz, 1H), 7.19 (m, 1H), 6.87 (d, $J$ = 7.2 Hz, 1H), 3.94 (s, 3H), 3.90 (s, 3H), 3.90 (s, 2H), 3.86 (s, 2H), 2.44 (s, 3H). $^{13}$C NMR (100 MHz, $CDCl_3$) $\delta$ 195.6, 158.2, 153.3, 148.9, 148.7, 136.7, 129.1, 123.6, 122.8, 122.3, 110.2, 110.0, 62.9, 62.6, 55.9, 55.8, 42.8. IR (thin film, cm$^{-1}$) 3006.5−2812.7, 1684.5, 1593.9, 1508.1, 1457.0, 1268.9, 1151.3, 1024.0. HRMS (+ESI): Calcd. for $MH^+$, 301.1552; Found, 301.1548.

**[Zn(DM-EBAP)($NO_3$)$_2$] (20).** Compound **17** (156 mg, 375 $\mu$mol) was dissolved in 3.0 mL of $H_2O$, and the pH was raised to >10 with 45% KOH. The oily mixture was extracted with $CH_2Cl_2$ (3 × 3 mL), and the organic fractions were combined, dried over anhydrous $Na_2SO_4$, and the solvent was removed to provide **16** as a colorless oil (83.5 mg, 82.7%). The free base **16** was dissolved in 1.00 mL of $CH_3CN$ to afford a 309 mM stock solution. An aliquot of the stock solution **16** (239 $\mu$L, 73.9 $\mu$mol) was combined with 3.0 mL of anhydrous $CH_3OH$ and 311 mM $Zn(NO_3)_2\cdot 6H_2O$ in $CH_3CN$ (262 $\mu$L, 81.5 $\mu$mol). The resulting solution was agitated briefly, allowed to stand at 23 °C for 30 min, and placed into an $Et_2O$ diffusion chamber where single crystals gradually formed from solution over 2 days. After harvesting a suitable crystal for X-ray crystallography, the remaining crystals were isolated by decanting the mother liquor, repeatedly washed with $Et_2O$ (3 × 5 mL), powdered and dried to constant weight under vacuum (20 mg, 60%). Anal. Calcd for $ZnO_6N_6C_{16}H_{22}$ (**20**): C, 41.80; H, 4.82; N, 18.28. Found: C, 41.69; H, 4.67; N, 17.95. IR (KBr pellet, cm$^{-1}$): 3113, 3074, 3003, 2974, 2899, 2819, 1605, 1572, 1460, 1427, 1321, 1084, 1030, 982, 818, 775, 731, 640, 594, 467, 422.

**General Spectroscopic Methods.** All solutions were prepared with spectrophotometric grade solvents. HEPES (4-(2-hydroxyethyl)-1-piperazineethanesulfonic acid), KCl (99.5%), and PAR (4-(2-pyridylazo)resorcinol, 99%) were purchased and used as received. $Zn^{2+}$ stock solutions were prepared from 99.999% pure $ZnCl_2$. All $Zn^{2+}$ solutions were standardized by titrating with terpyridine and measurement of the absorption spectra. ZinCleav-1 was introduced to aqueous solution by addition of stock solution in DMSO (3.33 mM). Graphs were manipulated and equations calculated by using Kaleidagraph 4.0. The pH values of solutions were recorded with an Omega PHB 212 glass electrode that was calibrated prior to each use. Absorption spectra were recorded on a Cary 50 UV−visible spectrophotometer under the control of a Pentium IV-based PC running the manufacturer supplied software package. Spectra were routinely acquired at 25 °C, in 1 cm path length quartz cuvettes with a total volume of 3.0 mL. Fluorescence spectra were recorded on a Hitachi F-4500 spectrophotometer under the control of a Pentium-IV PC running the FL Solutions 2.0 software package. Excitation was provided by a 150 W Xe lamp (Ushio Inc.) operating at a current of 5 A. Spectra were routinely acquired at 25 °C, in 1 cm quartz cuvette with a total volume of 3.0 mL using, unless otherwise stated, 5 nm slit widths and a photomultiplier tube power of 700 V. Photolysis experiments were performed at 25 °C, in 1 cm path length quartz cuvettes illuminated by a 150 W Xe lamp of a Hitachi F-4500 spectrophotometer with emission wavelength set to 350 or 360 nm. To obtain photoproducts for HPLC-MS analysis and to demonstrate the release of caged $Zn^{2+}$, solutions were placed in 1 cm path length quartz cuvettes and irradiated using a Rayonet photoreactor equipped with 8 bulbs each emitting at 3500 Å. High performance liquid chromatography (HPLC) was performed on a Shimadzu LC-10AT HPLC instrument connected to a Nova-Pak $C_{18}$ column (3.9 × 150 mm) and absorbance was measured at 254 nm. Potentiometric titrations were performed at 25 °C, using an Accument double junction electrode connected to an Oakton potentiometer.

**Determination of $Zn^{2+}$ Binding Constants. Calibration of the Electrode.** A solution of ~50 mM NaOH in 100 mM KCl was prepared and standardized by titrating against a 50.1 mM solution of potassium hydrogen phthalate using phenolphthalein as the indicator. The concentration of NaOH was determined to be 50.6 mM. A solution of ~50 mM HCl in 100 mM KCl was prepared and standardized by titrating against the 50.6 mM NaOH solution using phenolphthalein as the indicator. The concentration of HCl was determined to be 49.7 mM. A 20 mL aliquot of the 49.7 mM HCl solution was placed in a 100 mL beaker equipped with a magnetic stir bar. The electrode was immersed in the HCl solution, and the potential of the electrode was measured. 2.0 mL aliquots of the NaOH solution was added to the solution of HCl, and potential measurements were taken after each addition. The titration was continued until no change in potential occurs on the addition of NaOH. The potential of a pH electrode (E) is given by eq 1.

$$E = c' - \beta(0.05916)\mathrm{pH} \quad (1)$$

where $c'$ and $\beta$ are constants characteristic of a given pH electrode. A plot of $E$ versus pH yields $\beta$ as the gradient and $c'$ as the intercept.

**pH Titration.** A 10 mM solution of DM-EBAP·4HCl in 100 mM KCl was prepared. A 10 mL aliquot of the above solution was transferred to a 50 mL beaker equipped with a magnetic stir bar. The electrode was immersed in the DM-EBAP solution, and the potential of the electrode was measured. The above solution was titrated against a solution of 50.6 mM NaOH in 100 mM KCl. The potential of the DM-EBAP solution was measured after adding 250 $\mu$L aliquots of the NaOH solution and allowing ~5 min to equilibrate. The titration was continued until no further change in potential is observed upon addition of NaOH solution. Using eq 1, potential measurements were converted to pH values. The data was evaluated using Bjerrum's mathematical model for titration of a weak acid with a strong base. This yielded two p$K_a$ values (p$K_{a1}$ = 4.69, p$K_{a2}$ = 7.73) for DM-EBAP, from which the correction factor for ligand protonation was calculated to be 0.156.

**PAR Titration Procedure.** A 2.0 mL aliquot of a solution containing 4-(2-pyridylazo)resorcinol (PAR, 207 $\mu$M) at pH 7 (40 mM HEPES, 100 mM KCl) was placed in a cuvette and recorded as the background spectrum. A 2.0 $\mu$L aliquot of a $Zn^{2+}$ solution (9.02 mM) was added, and the UV−visible spectrum was recorded between 250 and 900 nm. The increase in absorbance at 500 nm results from the formation of $[Zn(PAR)_2]$ complex. Aliquots of the ZinCleav-1 stock solution (3.33 mM) were added in 1.0 $\mu$L increments, and the absorption spectra were recorded after each addition. The above procedure was repeated at 256 and 311 $\mu$M initial PAR concentrations to ensure reproducibility of results.

Since PAR forms both 1:1 and 1:2 complexes with $Zn^{2+}$, an excess of PAR that is sufficient to put >99% of the $Zn^{2+}$ bound to PAR in the $[Zn(PAR)_2]$ form must be used. Under these conditions, the binding equilibrium may be expressed by eq 2. The binding constant ($K'$) of the $[Zn(ZinCleav\text{-}1)]^{2+}$ complex may be obtained by solving eq 3.[25]

$$ZinCleav\text{-}1+PAR_2Zn = Zn(ZinCleav\text{-}1)+2PAR \quad (2)$$

$$\frac{[Zn(ZinCleav\text{-}1)][PAR]^2}{[ZinCleav\text{-}1][PAR_2Zn]} = \frac{K'}{\beta'_{PAR}} \quad \text{where} \quad \beta'_{PAR} = 2.2 \times 10^{12}\ M^{-1} \quad (3)$$

Equations 4−7 were used to calculate the individual components of eq 3.

$$[PAR_2Zn] = \frac{A_{500}}{\Delta\varepsilon_{500}} \quad \text{where} \quad \Delta\varepsilon_{500} = 6.6 \times 10^4 \quad (4)$$

$$[PAR] = [PAR]_{total} - 2[PAR_2Zn] \quad (5)$$

$$[Zn(ZinCleav\text{-}1)] = [PAR_2Zn]_{initial} - [PAR_2Zn] \quad (6)$$

$$[ZinCleav\text{-}1] = [ZinCleav\text{-}1]_{total} - [Zn(ZinCleav\text{-}1)] \quad (7)$$

$K'$ was calculated for each data point, averaged, and corrected for ligand protonation. The corrected binding constant was used to calculate the dissociation constant ($K_d$) of the $[Zn(ZinCleav\text{-}1)]^{2+}$ complex.

**Cu−Zn Exchange.** A 2.0 mL aliquot of a 60 $\mu$M solution of ZinCleav-1 (40 mM HEPES, 100 mM KCl, pH 7) was placed in a quartz cuvette, and a 12 $\mu$L aliquot of a $ZnCl_2$ stock solution (10 mM) was added to give final $Zn^{2+}$ concentration of 60 $\mu$M. A 24 $\mu$L aliquot of a $CuCl_2$ stock solution (50 mM) was added to give a final $Cu^{2+}$ concentration of 600 $\mu$M, and absorption spectra were recorded at 5 min intervals for 30 min.

**Photolysis of ZinCleav-1. Intensity of Source.** To determine the intensity of the radiation source, a 3.0 mL aliquot of a 6 mM potassium ferrioxalate solution was placed in a 1.0 cm path length quartz cuvette and irradiated with 350 nm wavelength radiation for 5 min while being stirred with a magnetic stir bar. This results in the reduction of Fe(III) oxalate to Fe(II) oxalate. The irradiated solution was combined with 26 mg of ferrozine (3 equiv) resulting in the formation of a reddish-purple solution containing $[Fe(ferrozine)_3]^{2+}$ which has a molar absorption coefficient of 27,900 $cm^{-1}\ M^{-1}$ at 563 nm. A 100 $\mu$L aliquot of the resulting solution was diluted by a factor of 30, and its absorbance was measured at 563 nm. The concentration of Fe(II) produced by the reduction of Fe(III) oxalate is given by eq 8.

$$[Fe(II)] = \frac{A_{563} \times 30}{\varepsilon_{563}} \quad \text{where} \quad \varepsilon_{563} = 27,900\ cm^{-1}\ M^{-1} \quad (8)$$

The intensity of the radiation source at 350 nm is given by eq 9.

$$\text{Intensity}(\text{quanta}\ s^{-1}\ L^{-1}) = \frac{[Fe(II)]/\text{Irradiation time}}{\Phi_{350}} N_A \quad \text{where} \quad \Phi = 1.26 \quad (9)$$

The above procedure was repeated with 360 nm wavelength radiation to determine the intensity of radiation source at 360 nm.

**Quantum Efficiency of Photolysis.** To determine the quantum efficiency of photolysis of ZinCleav-1, a 2.0 mL aliquot of DMSO or aqueous buffer was placed in a 1.0 cm path length quartz cuvette and a background UV−visible spectrum was recorded. A 36 $\mu$L aliquot of the ZinCleav-1 stock solution (3.33 mM) was added to give a final concentration of 60 $\mu$M. The cuvette was placed in the fluorescence spectrophotometer and irradiated at 350 nm while the solution was stirred with a magnetic stir bar. Absorption spectra of the solution were recorded at 5 min intervals. Spectra were acquired until no further changes in absorbance could be observed. The molar absorption coefficient at 300 nm for ZinCleav-1 ($\varepsilon_{ZnC}$) was determined to be 2,735 $cm^{-1}\ M^{-1}$ by applying the Beer−Lambert law to the spectrum of solution of ZinCleav-1 prior to photolysis. The molar absorption coefficient at 300 nm for **2** ($\varepsilon_{nitroso}$) was determined to be 3,470 $cm^{-1}\ M^{-1}$ by applying the Beer−Lambert law to the completely photolyzed ZinCleav-1 solution. The absorbance of the ZinCleav-1 solution at any time during photolysis is given by eq 10.

$$A_{total} = \varepsilon_{ZnC} l c_{ZnC} + \varepsilon_{nitroso} l c_{nitroso} \quad \text{where} \quad c_{ZnC} + c_{nitroso} = 60\ \mu\ M \quad (10)$$

Thus, the change of the concentration of ZinCleav-1 can be determined as a function of irradiation time.

The quantum efficiency of photolysis of ZinCleav-1 (QE) is obtained by solving eq 11 where $N_A$ is Avogadro's number.

$$\text{Quantum Efficiency} = \frac{\text{Change in } [ZinCleav\text{-}1]/\text{Irradiation time}}{\text{Intensity of the source}} \cdot N_A \quad (11)$$

Similarly, the quantum efficiency of photolysis of $[Zn(ZinCleav\text{-}1)]^{2+}$ was determined by irradiating 60 $\mu$M solution of $[Zn(ZinCleav\text{-}1)]^{2+}$ in DMSO and aqueous buffer.

**LC/MS Analysis of Mixtures.** To obtain photoproducts **2** and **3** for LC/MS analysis, a 1 mL aliquot of a 100 $\mu$M ZinCleav-1 solution was placed in a quartz cuvette and irradiated in a Rayonet RPR-100 photoreactor at 350 nm for 5 min. A 100 $\mu$L aliquot was injected in to the HPLC instrument, and the sample was eluted with 40% $CH_3OH$ in 2% aqueous $NH_4OAc$ at 300 $\mu$L $s^{-1}$. Compounds were detected by UV absorption at 254 nm. The 10 $\mu$L aliquots of the separated fractions were injected separately into the mass spectrometer. The same procedure was repeated with a 100 $\mu$M solution of $[Zn(ZinCleav\text{-}1)]^{2+}$.

**Release of Caged $Zn^{2+}$.** A 2.0 mL aliquot of a 20 $\mu$M ZP1B solution was placed in a quartz cuvette, and the fluorescence spectrum was recorded. An 8.9 $\mu$L aliquot of a $ZnCl_2$ stock solution (9.02 mM) was added to give a final concentration of 40 $\mu$M, and the fluorescence spectrum was recorded. A 24 $\mu$L

(25) Walkup, G. K.; Imperiali, B. *J. Am. Chem. Soc.* **1997**, *119*, 3443–3450.

**Table 1.** Crystallographic Parameters for [Zn(DM-EBAP)$(NO_3)_2$] (**20**)

| | |
|---|---|
| formula | $ZnO_6N_6C_{16}H_{22}$ |
| formula wt | 459.77 |
| space group | $P2_1/n$ |
| $a$, Å | 8.6057(2) |
| $b$, Å | 15.3221(4) |
| $c$, Å | 14.2571(4) |
| $\beta$, deg | 93.9123(17) |
| $V$, Å$^3$ | 1875.53(9) |
| $Z$ | 4 |
| $\rho_{calcd}$ (g/cm$^3$) | 1.628 |
| absorp. coeff. (cm$^{-1}$) | 22.629 |
| temp, K | 93 |
| total no. data | 12725 |
| obs data[a] | 3122 |
| no. parameters | 299 |
| R, %[b] | 0.0731 |
| wR2, %[c] | 0.1724 |
| max/min peaks, e/Å | 0.99, −0.83 |

[a] Observation criterion: $I > 2\sigma(I)$. [b] $R = \sum||F_o| - |F_c||/\sum|F_o|$. [c] wR2 = $[\sum w(F_o^2 - F_c^2)^2/\sum w(F_o^2)^2]^{1/2}$.

aliquot of the ZinCleav-1 stock solution (3.33 mM) was added to give a final concentration of 40 $\mu$M, and the fluorescence spectrum was recorded. The cuvette was irradiated in a Rayonet RPR-100 photoreactor with 350 nm wavelength radiation, and the fluorescence spectra were recorded at 2 min intervals.

**$^1$H NMR Titrations.** The $^1$H NMR spectrum of 2-(aminomethyl)pyridine in DMSO was recorded. A solution of $ZnCl_2$ in DMSO (1.50 mL, 6.4 mM) was placed in an NMR tube, and the $^1$H NMR spectrum was recorded. To this solution, aliquots of 2-(aminomethyl)pyridine were added, and $^1$H NMR spectra were recorded after each addition. The change in chemical shift of the methylene H's was monitored. The concentration of 2-(aminomethyl)pyridine after each addition was calculated. By performing non-linear regression analysis on the data,[26] the dissociation constants $K_{d1}$ and $K_{d2}$ were determined for the Zn:2-(aminomethyl)pyridine complex. The same procedure was repeated with ligands **3** and **18** to determine their respective dissociation constants.

**Collection and Reduction of X-ray Data.** Structural analysis was carried out in the X-Ray Crystallographic Facility at Yale University. Crystals were covered with oil, and a colorless plate of $ZnO_6N_6C_{16}H_{22}$ with approximate dimensions of 0.20 × 0.20 × 0.20 mm was mounted on a glass fiber at room temperature and transferred to a Rigaku RAXIS RAPID imaging plate area detector with graphite monochromated Cu K$\alpha$ radiation ($\lambda$ = 1.54187 Å) controlled by a PC running the Rigaku CrystalClear software package.[27] The data were collected at a temperature of −180 ± 1 °C to a maximum $2\theta$ value of 130.1°. The data were corrected for Lorentz and polarization effects. The structure was solved by direct methods[28] and expanded using Fourier techniques.[29] The space group was determined by examining systematic absences and confirmed by the successful solution and refinement of the structure. The non-hydrogen atoms were refined anisotropically. Hydrogen atoms were refined using the riding model. In the structure of **20**, both nitrate anions are disordered and were modeled and refined accordingly. All calculations were performed using the CrystalStructure[30] crystallographic software package except for refinement, which was performed using SHELXL-97.[28] Relevant crystallographic information is summarized in Table 1, and the 50% thermal ellipsoid plot is shown in Figure 2.

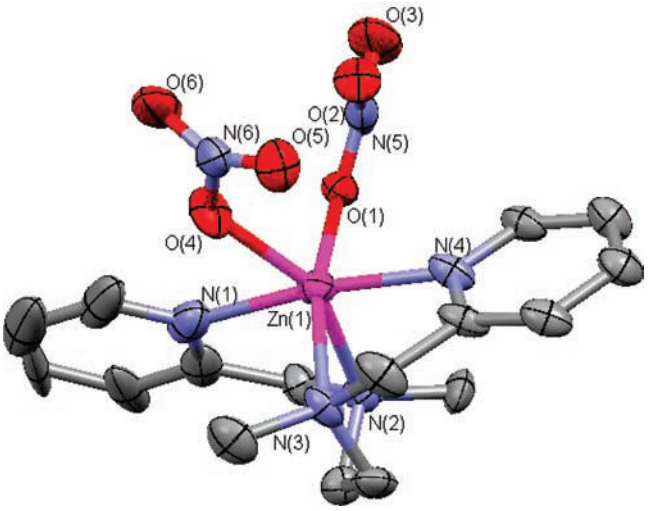


**Figure 2.** ORTEP diagram of ZinCleav-1 model complex [Zn(DM-EBAP)$(NO_3)_2$] (**20**) showing 50% thermal ellipsoids and selected atom labels. Hydrogen atoms are omitted for clarity.

## Results and Discussion

**Design and Synthesis.** We initially envisioned adapting a previously reported synthesis of an EDTA-based cage to make ZinCleav-1 and a variety of related ligands.[4] In the reported synthesis, a vicinal dibromide was reacted with diethyl iminodiacetate at high pressure (5000 psi) for extended periods of time (21 days) to provide a nitrobenzyl-based EDTA ligand in modest yield (<40%). In addition to the impractical and time-consuming techniques, this route only permits access to symmetric ligands derived from secondary amines. Alternatively we considered using the dibromide as a substrate in reactions; however, elimination reactions dominated the product distribution. Since this pathway failed to provide any useful strategies for preparing caged complexes, we devised a different route to the desired ligand starting with a Strecker synthesis (Scheme 1).

Starting with aldehyde **4**, α-aminonitrile **5** was prepared. Attempts to access a diamine by reduction of **5** resulted in loss of the nitrile group; however, hydrolysis of **5**, followed by a sequence of simple synthetic manipulations provided the protected amino alcohol **9**. Installation of a carbamate on the benzylic nitrogen atom appears to stabilize the intermediates to unwanted decomposition reactions, and this chemistry is being examined to optimize and shorten our synthetic route. Using Dess-Martin periodinane, **9** was converted to the corresponding aldehyde **10** in 22% overall yield for the 6 step sequence. Since the individual reactions occur under mild conditions, are all high yielding, and require minimal purification, multigram quantities of the versatile synthetic intermediate **10** can be accessed readily in less than 5 days.

Our initial design of ZinCleav-1 was based on ethylene-bis-α,α′-(2-aminomethyl)pyridine (EBAP), a chelator which has a high affinity for $Zn^{2+}$ ($K_d$ = 3.1 pM), as well as several other first row transition metals like $Cu^{2+}$ ($K_d$ = 0.05 fM), $Ni^{2+}$ ($K_d$ = 0.20 pM), and $Co^{2+}$ ($K_d$ = 0.16 pM);[22] and like

(26) Connors, K. A., *Binding Constants: The Measurements of Molecular Complex Stability*; John Wiley and Sons: NJ, 1987; p 432.
(27) *CrystalClear and CrystalStructure*; Rigaku/MSC: The Woodlands, TX, 2005.
(28) Sheldrick, G. M. *SHELX97*, 1997.
(29) Beurskens, P. T.; Admiraal, G.; Beurskens, G.; Bosman, W. P.; de Gelder, R.; Israel, R.; Smits, J. M. M. *DIRDIF99*; University of Nijmegen: The Netherlands, 1999.
(30) *CrystalStructure 3.8: Crystal Structure Analysis Package*; Rigaku and Rigaku Americas: The Woodlands, TX, 2007.

**Scheme 1.** Synthesis of ZinCleav-1

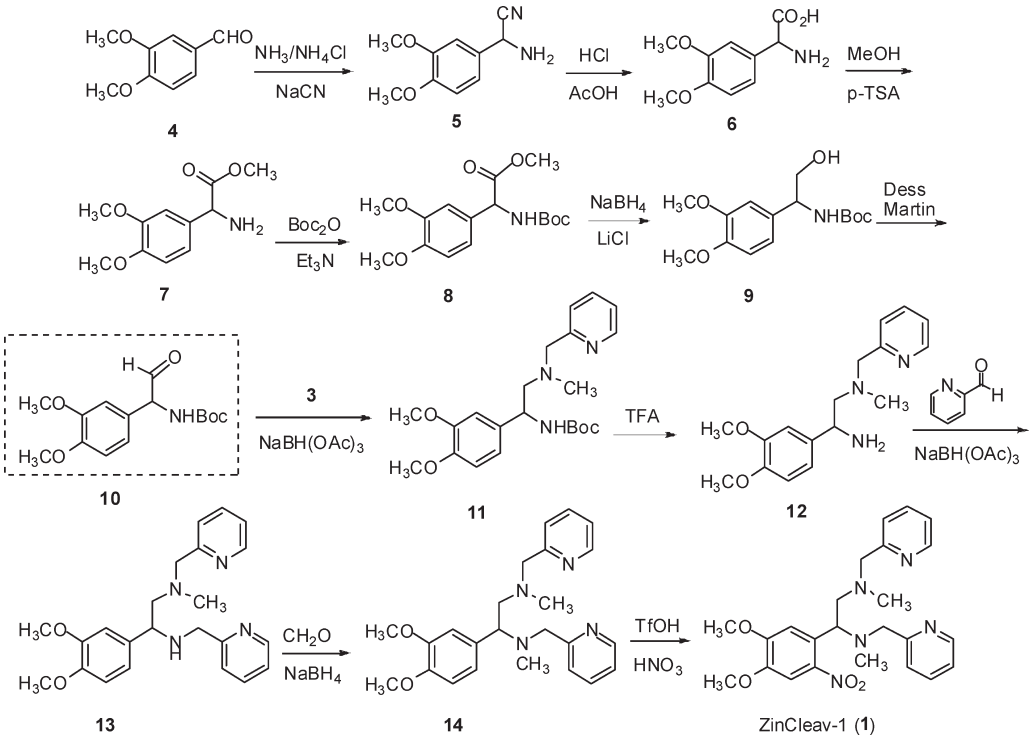


the common chelator *N*,*N*,*N*′,*N*′-tetrakis-(2-pyridylmethyl)-ethylenediamine (TPEN), the combination of pyridyl and amine ligands minimizes its binding affinity for $Ca^{2+}$ and $Mg^{2+}$. With aldehyde **10**, one *N*-methyl-2-aminopyridyl ligand was introduced using reductive amination to provide **11**. After removal of the carbamate protecting group, the second pyridyl ligand was installed and methylated with two successive reductive amination reactions using 2-pyridine carboxaldehyde and formaldehyde, respectively, to provide **14**, a stable precursor of ZinCleav-1. Introduction of the nitro group in the final step of the reaction sequence limits the handling and manipulation of photoactive compounds, and will allow easy access to a diverse array of caged $Zn^{2+}$ complexes. While several standard nitration methods provided low yields of the desired compound, using the nitrating adduct derived from triflic acid (TfOH) and fuming nitric acid provided ZinCleav-1 in 39% yield.[31]

**Zinc Binding Studies.** The measured binding constants for the structurally similar EBAP ligands suggested that ZinCleav-1 would have a pM affinity for $Zn^{2+}$. Since the $[Zn(ZinCleav\text{-}1)]^{2+}$ lacks an adequate spectroscopic signature that changes with metal ion concentrations, the conditional binding constant was analyzed by competitive titration between the 4-(2-pyridyl-2-azo) resorcinol (PAR) $Zn^{2+}$ complex and ZinCleav-1. PAR forms a 2:1 L/M complex with a $\lambda_{max}$ at ~500 nm with $Zn^{2+}$ and has a $K_d$ of 0.5 pM at pH 7 (Figure 3).[32] Under simulated physiological conditions, titration of the $[Zn(PAR)_2]$ complex with ZinCleav-1 provided adequate spectroscopic information to evaluate affinity. Preliminary analysis of the PAR data, which was acquired in triplicate, provided a conditional binding constant of 1.5 pM. To correct this value for ligand protonation, *N*,*N*′-dimethyl-*N*,*N*′-bis-(2-pyridinylmethyl)ethane-1,2-diamine (DM-EBAP) was prepared, and its p$K_a$ values were obtained by potentiometic titration. The titration allowed an $\alpha$ value of 0.16 to be calculated, which provided $K_d$ of $0.23 \pm 0.04$ pM as the corrected apparent binding constant of ZinCleav-1 for $Zn^{2+}$ at pH 7 (Table 2).

Additional PAR titrations were performed with EBAP and DM-EBAP to confirm the validity of the PAR methodology by comparing these binding constants to those measured for EBAP by potentiometric titration.[22] The apparent $K_d$ of EBAP at pH 7 was determined to be 5.0 pM using PAR titration, which is consistent with the value obtained from potentiometric data, 3.1 pM. Although potentiometric studies demonstrate that EBAP binds more tightly to $Cu^{2+}$ as predicted by the Irving–Williams series,[22] treating $[Zn(ZinCleav\text{-}1)]^{2+}$ with a 10-fold excess $Cu^{2+}$ showed only a slow ligand exchange reaction. Only 10% of the $Zn^{2+}$ atoms are displaced by $Cu^{2+}$ over a period of 10 min. Since the exchange rate is slow and the concentration of free $Cu^{2+}$ in cells is low, the only metal uncaged when biological specimens are treated with $[Zn(ZinCleav\text{-}1)]^{2+}$ should be $Zn^{2+}$.

**Structural Studies.** Multiple structural isomers of dipyridylethylene diamine complexes related to EBAP have been observed in the solid state.[33] We obtained X-ray quality crystals of the ZinCleav-1 model DM-EBAP to support our complex formulation, and the structure of **20** is displayed in Figure 2 as an Oak Ridge Thermal Ellipsoid Plot (ORTEP) diagram. Details of the X-ray analysis are furnished in Table 1, and selected bond distances and angles are provided in Table 3. The model ligand was preferable for evaluating the structure since

(31) Coon, C. L.; Blucher, W. G.; Hill, M. E. *J. Org. Chem.* **1973**, *38*, 4243–4248.
(32) Tanaka, M.; Funahashi, S.; Shirai, K. *Inorg. Chem.* **1968**, *7*, 573–578.
(33) Ng, C.; Sabat, M.; Fraser, C. L. *Inorg. Chem.* **1999**, *38*, 5545–5556.

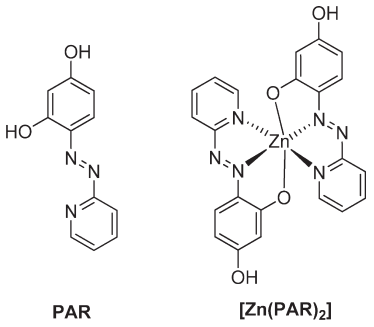


**Figure 3.** Structure of PAR and the [Zn(PAR)$^2$] complex.

**Table 2.** Binding Properties of Reported Chelators

| Ligand | p$K_a$ | $K_d$ | $K_d$ (PAR) |
|---|---|---|---|
| ZinCleav-1 (**1**) | a | - | 0.23 pM [a] |
| (**3**) [b] | p$K_{a1}$ = 1.40 [49]<br>p$K_{a2}$ = 8.88 | 194 μM (1:1)<br>1.34 mM (1:2) | c |
| 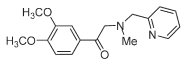 (**18**) [b, d] | - | 257 μM(1:1)<br>3.02 mM (1:2) | c |
| 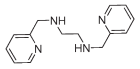 EBAP (**15**) | p$K_{a1}$ = 5.45 [50]<br>p$K_{a2}$ = 8.23 | 3.1 pM [22] | 5.0 pM |
| 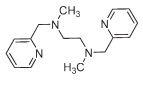 DM-EBAP (**16**) | p$K_{a1}$ = 4.69 [e]<br>p$K_{a2}$ = 7.73 | - | 1.6 pM |

[a] The dissociation constant of the [Zn(ZinCleav)]$^{2+}$ complex was corrected for ligand protonation using p$K_a$ values measured for **16**. [b] Binding affinity of **3** and **18** was assessed by NMR titration in DMSO-$d_6$ because of limited solubility in $D_2O$, and the lack adequate changes in the absorption spectra. [c] Binding affinities are too weak to be measured by competitive titration. [d] Ligand **18** was used as an analogue of **2** in NMR titrations. [e] The p$K_a$ values of **16** were measured by potentiometric titration. Competitive ligand titrations were performed with 207 μM PAR, 10 μM $ZnCl_2$, 40 mM HEPES, 100 mM KCl, pH 7.

ZinCleav-1 is prepared as a racemic mixture of *R* and *S* isomers at the benzylic carbon atom. While the stereochemistry will not affect the chelation properties, obtaining single crystals from such mixtures can be challenging. In the structure of the model complex, the $Zn^{2+}$ adopts a distorted octahedral geometry with the pyridine ligands occupying the axial coordination sites. The complex crystallizes as the $C_2$ symmetric cis α isomer, which seems to be favored for ethylene diamine ligands with tertiary amines and 5-membered chelate rings.[35,36] Similar mononuclear complexes have been reported with divalent iron[23,37,38] and manganese.[39] The crystals were obtained from an $Et_2O$ diffusion into an $CH_3OH/CH_3CN$ solution containing the complex derived from $Zn(NO_3)_2$. Attempts to obtain complexes from either $ZnCl_2$ or $Zn(ClO4)_2$ failed to obtain X-ray quality crystals. Under buffered aqueous conditions used in the spectroscopy, the nitrate ligands that occupy the remaining equatorial sites will probably replaced by either a chloride or a water ligand.

**Table 3.** Selected Interatomic Distances (Å) and Angles (deg) for [Zn(DM-EBAP)$(NO_3)_2$] (**20**)

| bond lengths | | bond angles | |
|---|---|---|---|
| Zn(1)−N(1) | 2.161(6) | N(1)−Zn(1)−N(4) | 171.6(2) |
| Zn(1)−N(2) | 2.214(5) | N(1)−Zn(1)−N(2) | 76.6(2) |
| Zn(1)−N(3) | 2.187(5) | N(1)−Zn(1)−N(3) | 99.8(2) |
| Zn(1)−N(4) | 2.145(5) | N(2)−Zn(1)−N(3) | 82.20(19) |
| Zn(1)−O(1) | 2.170(10) | N(2)−Zn(1)−N(4) | 95.08(19) |
| Zn(1)−O(4) | 2.092(9) | N(3)−Zn(1)−N(4) | 77.3(2) |
| | | O(1)−Zn(1)−O(4) | 96.5(3) |
| | | O(1)−Zn(1)−N(2) | 85.1(3) |
| | | O(1)−Zn(1)−N(3) | 164.8(3) |
| | | O(1)−Zn(1)−N(4) | 95.7(3) |
| | | O(4)−Zn(1)−N(1) | 73.6(3) |
| | | O(4)−Zn(1)−N(2) | 149.9(2) |
| | | O(4)−Zn(1)−N(3) | 98.7(2) |
| | | O(4)−Zn(1)−N(4) | 114.6(3) |

[a] Number in parentheses are estimated standard deviations in the last digit(s). Atom labels are provided in Figure 2.

**Photochemistry.** To assess the photochemistry of the new caged complexes, ZinCleav-1 and [Zn(ZinCleav)]$^{2+}$ were irradiated with a 150 W xenon lamp, and the intensity of the radiation source was measured by iron oxalate actinometry.[40] Photolysis of ZinCleav-1 was performed by exposing a 60 μM solution of the ligand in buffer to 350 nm light for 65 min. The $\lambda_{max}$ of [Zn(ZinCleav-1)]$^{2+}$ was red-shifted to 360 nm, and completion of the photolysis required additional irradiation time. Completion of the photoreaction was determined by monitoring changes in the UV−vis spectrum and analyzing the reaction mixtures by LC-MS. The photolysis also was carried out in DMSO to verify the values obtained in aqueous solution because secondary changes were observed in the absorption spectra, presumably resulting from hydrolytic chemistry of the nitroso species; however, the calculated quantum yields were nearly identical regardless of the medium. The quantum efficiency of photolysis of ZinCleav-1 and its metal complex were calculated to be 2.4% and 0.55%, respectively, using the extinction coefficients of ZinCleav-1 and its photoproduct **2** to calculate conversion with respect to time. Unexpectedly, the $Zn^{2+}$ had a lower quantum yield than the apo-ligand in contrast to the structurally related EDTA cage that exhibits the opposite trend.[4] We hypothesize that the *N*-methyl group may partially block the abstraction of the benzylic hydrogen atom that initiates the cleavage reaction. Future efforts will focus on optimizing the uncaging efficiency of our complexes by systematically correlating structural features with the quantum yields. In addition, while electron donating groups on the nitrobenzyl ring red shift excitation, which helps prevent photodamage of biological specimens,

(34) Alderighi, L.; Gans, P.; Ienco, A.; Peters, D.; Sabatini, A.; Vacca, A. *Coord. Chem. Rev.* **1999**, *184*, 311–318.
(35) Fenton, R. R.; Stephens, F. S.; Vagg, R. S.; Williams, P. A. *Inorg. Chim. Acta* **1991**, *182*, 67–75.
(36) Glerup, J.; Goodson, P. A.; Hodgson, D. J.; Michelsen, K. *Inorg. Chem.* **1995**, *34*, 6255–6264.
(37) Taktak, S.; Kryatov, S. V.; Rybak-Akimova, E. V. *Inorg. Chem.* **2004**, *43*, 7196–7209.
(38) Taktak, S.; Flook, M.; Foxman, B. M.; Que, L.; Rybak-Akimova, E. V.; Akimova, R. *Chem. Commun.* **2005**, 5301–5303.
(39) Hureau, C.; Blondin, G.; Charlot, M. F.; Philouze, C.; Nierlich, M.; Cesario, M.; Anxolabehere-Mallart, E. *Inorg. Chem.* **2005**, *44*, 3669–3683.
(40) Hatchard, C. G.; Parker, C. A. *Proc. R. Soc., London, Ser. A* **1956**, *235*, 518–536.

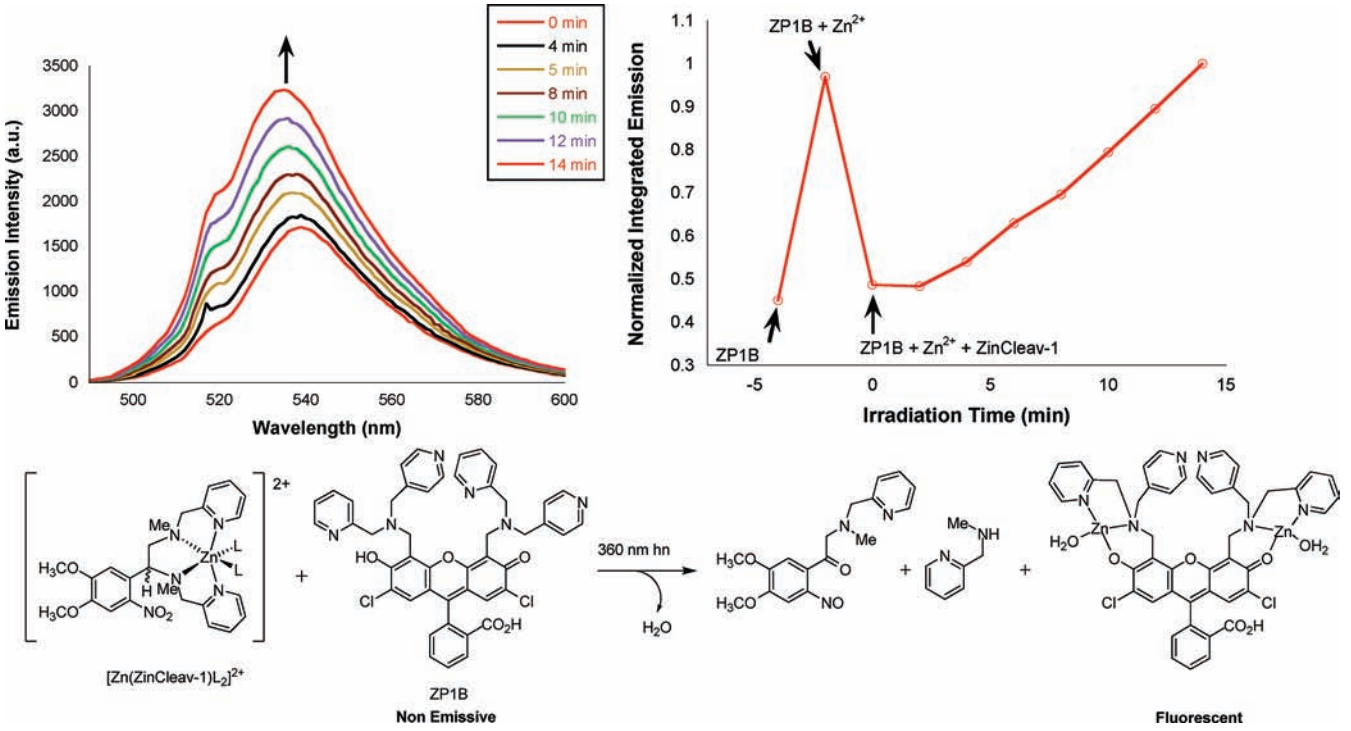


**Figure 4.** Fluorescence response of ZP1B upon uncaging of ZinCleav-1 (top left). The emission intensity of a solution of 20 $\mu$M ZP1B (40 mM HEPES, 100 mM KCl, pH 7) was recorded before and after the addition of 40 $\mu$M $ZnCl_2$. The emission was integrated between 490 and 600 nm and normalized to the maximum response (top right). Subsequent addition of 40 $\mu$M ZinCleav-1 quenched the emission of the ZP1B complex, which has a $K_d$ of 13 $\mu$M for $Zn^{2+}$. Irradiation of the solution in a Rayonet RPR-100 photoreactor resulted in a complete photolysis of ZinCleav-1 within 15 min. This behavior is consistent with ZP1B acquiring $Zn^{2+}$ from the photolyzed ZinCleav-1 (bottom).

these substituents also promote the formation of charge transfer states that compete with the desired photochemical processes, which decreases the quantum yield of uncaging.[41]

Analysis of the photoreaction of ZinCleav-1 by LC-MS revealed the disappearance of the ligand upon irradiation and the simultaneous appearance of photoproducts **2** and **3**. To determine the probable $Zn^{2+}$ speciation after photolysis, the binding affinities of the two predominant photoproducts for $Zn^{2+}$ were measured by $^1$H NMR in DMSO-$d_6$. Compound **17** was used as a model for **2** since the nitroso compound could not be prepared independently. Limited solubility of the compounds in aqueous solution precluded NMR experiments in $D_2O$, and like ZinCleav-1 the photoproducts lack an adequate inherent spectroscopic signature when titrated with $Zn^{2+}$. Unlike the intact cage, the photoproducts' binding affinities are too weak for competitive titrations with PAR. Under the conditions of the titration, both ligands form 1:1 and 1:2 M/L complexes with a $K_d > 150\,\mu$M for the 1:1 complexes and a 1:2 binding constant in the mM range. The latter binding constant is too weak to be relevant under physiological conditions.

We further assessed the nature of the weakly bound $Zn^{2+}$ complexes by uncaging the complex in the presence of the fluorescent sensor ZP1B, which has a $K_d$ of 13 $\mu$M for $Zn^{2+}$.[42] Addition of 40 $\mu$M ZnCleav-1 to a solution containing 40 $\mu$M $Zn^{2+}$ and 20 $\mu$M ZP1B leads to an immediate extinguishing of the fluorescence enhancement that was observed when the sensor and metal ion were mixed. Upon irradiation of the solution in an intense 600 W light source, the ligand is completely photolyzed after 15 min as indicated by the complete restoration of the emission intensity (Figure 4). Although no loss in emission intensity was observed qualitatively, the extent of fluorescein photobleaching would need to be measured to use such experiments quantitatively. While the cage is cleaved relatively slowly even with an intense source or radiation, the ligand exchange between the photoproducts and the sensor appears to be fast. The emission intensity was measured immediately after removing the cuvette from the photoreactor at regular intervals, and no additional change in intensity was observed until after additional irradiation. This behavior is consistent with the fragmentation of the ZinCleav-1 backbone and the formation of photoproducts that bind $Zn^{2+}$ with lower affinity than ZP1B.

**Application Considerations.** Using these binding affinities and the typical uncaging efficiency of nitrobenzyl compounds by flash photolysis, accessible changes in free [$Zn^{2+}$] were calculated for two different scenarios (Table 4). Flash photolysis provides a high intensity burst of light that mitigates the slow and inefficient uncaging observed with traditional light sources.[43] For entries 2−7 only the equilibrium between ZinCleav, $Zn^{2+}$, and the photoproducts are considered. By fixing the concentration of ZinCleav-1 at 50 $\mu$M and varying the total [$Zn^{2+}$] between 33 and 50 $\mu$M, equilibrium free [$Zn^{2+}$] between 0.5 pM and 3.5 nM are accessible; however, free metal ion concentrations are very sensitive to perturbation in the amounts of chelator and total $Zn^{2+}$. Such sensitivity would

(41) Bochet, C. G. *Tetrahedron Lett.* **2000**, *41*, 6341–6346.
(42) Wong, B. A.; Friedle, S.; Lippard, S. J. *Inorg. Chem.* **2009**, *48*, ASAP, DOI: 10.1021/ic900990w.
(43) Gurney, A. M.; Lester, H. A. *Physiol. Rev.* **1987**, *67*, 583–617.

**Table 4.** Free $[Zn^{2+}]$ Buffering Using ZinCleav-1[a]

| resting $[Zn^{2+}]$ | added [ZinCleav-1] | added $[Zn^{2+}]$ | $[Zn^{2+}]$ with 10% uncaging | $[Zn^{2+}]$ with 25% uncaging | $[Zn^{2+}]$ with 50% uncaging |
|---|---|---|---|---|---|
| 749 pM[b,45] | 50 $\mu$M | 50 $\mu$M | 764 pM[c] | 1.3 nM[c] | 7.6 nM[c] |
| 0.50 pM[d] | 50.0 $\mu$M | 33.2 $\mu$M | 0.53 pM | 1.9 pM | 3.8 $\mu$M |
| 1.0 pM[d] | 50.0 $\mu$M | 40.0 $\mu$M | 1.1 pM | 1.6 $\mu$M | 7.3 $\mu$M |
| 5.0 pM[d] | 50.0 $\mu$M | 47.6 $\mu$M | 8.5 pM | 6.6 $\mu$M | 11.4 $\mu$M |
| 10 pM[d] | 50.0 $\mu$M | 48.8 $\mu$M | 61.3 pM | 7.4 $\mu$M | 12.1 $\mu$M |
| 25 pM[d] | 50.0 $\mu$M | 49.5 $\mu$M | 476 nM | 7.8 $\mu$M | 12.5 $\mu$M |
| 42 pM[d] | 50.0 $\mu$M | 49.7 $\mu$M | 667 nM | 8.0 $\mu$M | 12.7 $\mu$M |
| 3.5 nM[d] | 50.0 $\mu$M | 50.0 $\mu$M | 953 nM | 8.2 $\mu$M | 12.8 $\mu$M |

[a] Speciation was simulated and concentrations were calculated with HySS.[34] ZinCleav-1 photoproducts were assumed to have $-\log \beta = 4.4$. [b] Reported resting free $[Zn^{2+}] = 784$ pM; calculations are based on a total cellular $[Zn^{2+}] = 264$ $\mu$M and cellular chelators with collective $K_d = 83$ pM. [c] The increase in free $[Zn^{2+}]$ concentration is illustrated in Figure 5. [d] Free $[Zn^{2+}]$ do not assume any external buffering.

require the ability to accurately determine the amount of each species added to solution to achieve these exact free $[Zn^{2+}]$. For intracellular applications, the loading of cage into cells would need to be measured as has been reported for $Zn^{2+}$ sensors.[44] Photolysis dramatically increases the free $[Zn^{2+}]$. While such models are illustrative generally, application of caged complexes to biological problems requires a detailed knowledge of the system being investigated.

While many measurements of free $[Zn^{2+}]$ in different cell lines have been reported, the corresponding exact total cellular $[Zn^{2+}]$ and the concentration of biological $Zn^{2+}$ chelators of specific cells have received less attention. Recently Krezel and Maret provided a detailed description of $Zn^{2+}$ content and equilibria in human colon cancer cells.[45] By digesting the cells with acid, a total cellular $[Zn^{2+}]$ of 264 $\mu$M was measured, and additional experiments demonstrated a total cellular $K_d = 85$ pM. With this detailed information, it is possible to calculate the amount of ZinCleav-1 and exogenous $Zn^{2+}$ required to maintain intracellular homeostasis. In these calculations, $Zn^{2+}$ binding to intracellular proteins are accounted for by treating the cell as a simple ligand (Table 4, entry 1). In contrast to the calculations described above, a narrower range of resting $[Zn^{2+}]$ is accessible because of the additional buffering by endogenous ligands. Subsequent uncaging of ZinCleav-1 will transiently increase the free $[Zn^{2+}]$ and initiate cellular responses to reestablish equilibrium. As shown in Figure 5, the most dramatic increases are observed when >25% of the caged complex is photolyzed; however, since $Zn^{2+}$ is typically under tight regulation, even a modest increase in free $[Zn^{2+}]$ will likely elicit a significant response. The speciation plot also illustrates the instantaneous composition of zinc complexes in solution. The weakly binding photoproducts (photoprod = **2** and **3** collectively) will readily exchange with the high affinity cellular sites.

Future investigations will focus on developing techniques to employ ZinCleav-1 in biological studies. In particular, the biodistribution and method of administration of ZinCleav-1 will need to be established. While $[Zn(ZinCleav-1)]^{2+}$ should be membrane impermeable owing to its charge, the apo ligand should freely cross cell membranes. While complex impermeability would be an advantage in extracellular studies or if the complex was microinjected into cells, any apo ligand used for buffering could translocate and perturb buffering if membrane permeability is fast compared to the experimental time frame.

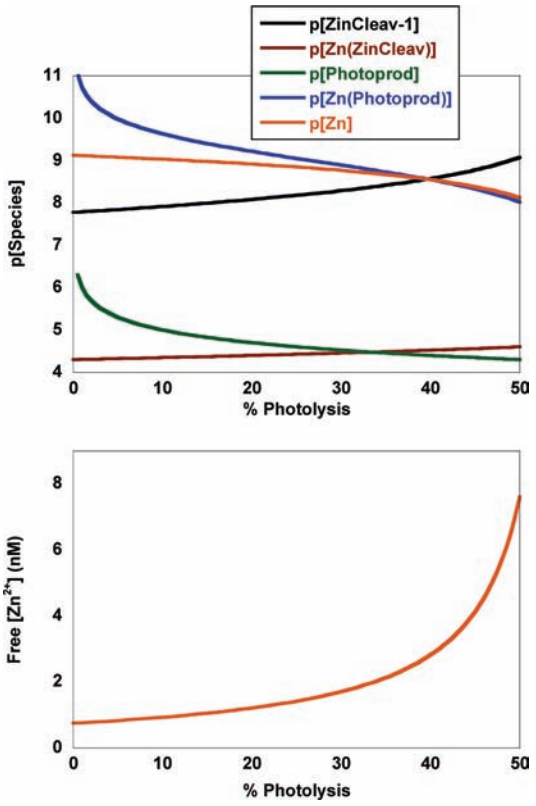


**Figure 5.** Speciation of various components in solution upon photolysis of ZinCleav-1 (top) and the corresponding changes in free $[Zn^{2+}]$ (bottom) calculated using HySS.[34] Calculations are based on adding 50 $\mu$M ZinCleav-1 and 50 $\mu$M $Zn^{2+}$ to a buffered system with a total cellular $[Zn^{2+}] = 264$ $\mu$M and cellular chelators with collective $K_d = 83$ pM as described for entry 1 in Table 4. The p[species] represents the $-\log$[species], and the Photoprod corresponds collectively to compounds **2** and **3** formed upon ZinCleav-1 photolysis.

## Conclusions

The participation of chelatable $Zn^{2+}$ in brain function[46] and disease[47] remains enigmatic. The current theory that synaptic $Zn^{2+}$ participates in neurotransmission has yet to be

(44) Aoki, S.; Sakurama, K.; Ohshima, R.; Matsuo, N.; Yamada, Y.; Takasawa, R.; Tanuma, S. I.; Talkeda, K.; Kimura, E. *Inorg. Chem.* **2008**, *47*, 2747–2754.
(45) Krezel, A.; Maret, W. *J. Biol. Inorg. Chem.* **2006**, *11*, 1049–1062.
(46) Vogt, K.; Mellor, J.; Tong, G.; Nicoll, R. *Neuron* **2000**, *26*, 187–196.
(47) Angel, I.; Bar, A.; Horovitz, T.; Taler, G.; Krakovsky, M.; Resnitsky, D.; Rosenberg, G.; Striem, S.; Friedman, J. E.; Kozak, A. *Drug Dev. Res.* **2002**, *56*, 300–309.

proven irrefutably,[48] but $Zn^{2+}$ does possess properties common to all neuromodulators.[11] Since existing techniques for introducing $Zn^{2+}$ into biological systems can overwhelm a system with ionic $Zn^{2+}$, a physiologically irrelevant response may be induced inadvertently. ZinCleav-1 can provide control necessary to study the functions of $Zn^{2+}$ in biological experiments. ZinCleav-1 was accessed by a modular synthetic pathway that will allow additional caged complex candidates to be prepared. Caged ZinCleav-1 has a pM affinity for $Zn^{2+}$ that decreases by 9 orders of magnitude upon uncaging. Our future efforts will focus on using our new synthetic methods to prepare additional ZinCleav derivatives with properties tailored for specific applications and optimizing the uncaging efficiency as well as using ZinCleav-1 to study the chemistry of free $Zn^{2+}$ in biology.

**Acknowledgment.** This work was supported by the University of Connecticut. We thank C. V. Kumar for the use of HPLC and photoreactor instrumentation. We thank B. Wong and Prof. S. J. Lippard for the generous donation of ZP1B

**Supporting Information Available:** $^{1}H$ and $^{13}C$ NMR spectra for new compounds. Figure S-1 showing absorbance spectrum from the competitive titration of $[Zn(PAR)_2]$. Figures S-2 and S-3 showing the absorption changes upon uncaging of ZinCleav-1 and $[Zn(ZinCleav\text{-}1)]^{2+}$. Figures S-4, S-5, S-6, and S-7 showing the HPLC trace of the photoreaction and the MS of each component. Figures S-8, S-9, and S-10 showing the NMR titration data for the photoproducts. Figure S-11 showing the pH titration of DMEBAP. Figure S-12 showing the $Cu^{2+}$ exchange with $[Zn(ZinCleav\text{-}1)]^{2+}$ by UV−vis spectroscopy. Complete tables of X-ray data and fully labeled ORTEP diagram. This material is available free of charge via the Internet at http://pubs.acs.org.

(48) Colvin, R. A; Fontaine, C. P.; Laskowski, M.; Thomas, D. *Eur. J. Pharmacol.* **2003**, *479*, 171–185.

(49) Fischer, A.; King, M. J.; Robinson, F. P. *Can. J. Chem.* **1978**, *56*, 3059–3067.

(50) Gruenwedel, D. W. *Inorg. Chem.* **1964**, *3*, 495–501.